Type of contribution:
Editorial
▶ Research Paper
Case Study
Review Paper
Scientific Data
Report of Tech. Application

mesi e-issn. 2798-5245

Mechanical Engineering for Society and Industry
Vol. 5, No. 1 (2025) pp 182-189
https://doi.org/10.31603/mesi.12843

Stress distribution on the L1/L2 endplates under multiaxial loads: A finite element study

Hasyid Ahmad Wicaksono[1,2], Muhammad Rafli[1,2], Muhamad Bilal[1,2], M. Danny Pratama Lamura[1,2,3], Mohamad Izzur Maula[1,2,4], Athanasius Priharyoto Bayuseno[1], Tri Indah Winarni[2,5,6], Jamari[1,2*]

[1] Department of Mechanical Engineering, Faculty of Engineering, Universitas Diponegoro, Semarang 50275, Central Java, **Indonesia**
[2] Undip Biomechanics Engineering & Research Centre (UBM-ERC), Universitas Diponegoro, Semarang 50275, Central Java, **Indonesia**
[3] Department of Mechanical Engineering, Faculty of Engineering and Science, Universitas Pembangunan Nasional Veteran Jawa Timur, Surabaya 60294, East Java, **Indonesia**
[4] Department of Manufacturing Engineering Technology, Akademi Inovasi Indonesia, Salatiga 50721, Central Java, **Indonesia**
[5] Department of Anatomy, Faculty of Medicine, Universitas Diponegoro, Semarang 50275, Central Java, **Indonesia**
[6] Center for Biomedical Research (CEBIOR), Faculty of Medicine, Universitas Diponegoro, Tembalang, Semarang 50275, Central Java, **Indonesia**
✉ j.jamari@gmail.com

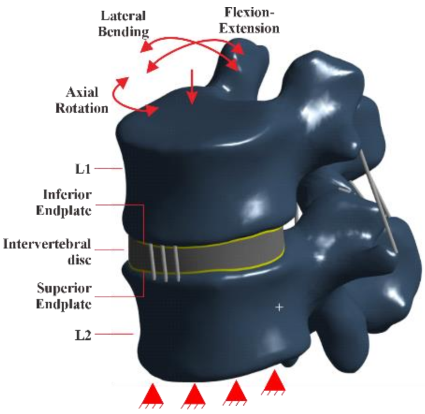

Highlights:

- Finite element analysis reveals highest von Mises stress on the L1/L2 superior endplate, especially during flexion and lateral bending.
- Extension movements significantly reduce stress levels by over 60%.
- Stress distribution is asymmetrical, influenced by cortical thickness and trabecular alignment.
- Findings highlight the superior endplate's vulnerability, crucial for implant design and fracture prevention.

Abstract

Understanding stress distribution on lumbar vertebral endplates is essential for predicting mechanical failure and guiding clinical interventions. Therefore, this study aims to investigate the von Mises stress patterns on the L1/L2 endplates under multiaxial loading using a 3-dimensional finite element (FE) model derived from CT imaging of a healthy 55-year-old male. Anatomical structures were reconstructed in Mimics 21.0, and simulations were conducted in ANSYS Workbench 2023 R2. Material properties for cortical bone, cancellous bone, and intervertebral disc were assigned based on validated biomechanical data. A compressive load of 500 N and multiaxial moments ranging from 2.5 to 10 N•m were applied to simulate physiological movements, while the inferior surface of L2 was fully constrained to reflect realistic boundary conditions. The results showed that the superior endplate experienced the highest von Mises stress, particularly during flexion and lateral bending, indicating increased vulnerability to mechanical overload. Extension loading significantly reduced stress on both endplates, with a 60.54% decrease on the superior endplate and 69.17% on the inferior endplate. Stress distribution was asymmetrical and was influenced by anatomical features, such as cortical thickness and trabecular alignment. These results show the superior endplate as a biomechanically critical region prone to degeneration, emphasizing its importance in implant design, preventive strategies, and risk assessment for microfracture in high-risk populations.

Keywords: Finite element analysis; Lumbar spine; Multiaxial loading; Endplate stress; L1–L2 segment

Article info
Submitted: 2024-12-18
Revised: 2025-06-26
Accepted: 2025-06-07

Publisher
Universitas Muhammadiyah Magelang

1. Introduction

Physical activities, such as walking and Salat (Islamic prayer) require a complex interplay of joint movements and load-bearing mechanisms within the human musculoskeletal system. Some of the most critical components during these activities are the hip joint and the vertebral column, which are responsible for transmitting and supporting significant mechanical loads. Previous studies have shown that the hip joint experiences high stress during walking [1], indicating the need for prosthetic hip designs to accommodate the unique postures performed during Salat [2]. The vertebral column plays a central role in maintaining posture, distributing body weight, and stabilizing movement. Anatomically, the vertebral column consists of several interconnected regions, including the cervical, thoracic, lumbar, sacral, and coccygeal segments, which are arranged in a continuous and orderly manner [3]. The lumbar spine (L1–L5), located between the thoracic spine and the pelvis, is essential for supporting upper body weight and enabling dynamic motion during daily physical activities [4].

During physical activities, there is a direct push or pull interaction between the complex structures and the supporting elements of the lumbar spine (L1–L5). Engaging in extreme activities may lead to injury of the structures, particularly in older adults. Previous studies showed that individuals aged 49–69 years were at increased risk for developing lumbar spondylosis [5]. This condition can significantly affect the lumbar spine structures, leading to degenerative disorders. The progression of lumbar spondylosis may further lead to degenerative disc disease and the formation of new bone growths (osteophytes) [6]. The condition can progress to lumbar spondylolisthesis, a condition characterized by the displacement of one vertebra, compressing the spinal nerves and surrounding tissues. A study by Yamamoto *et al*. [7] using in vitro testing provided valuable data on spinal range of motion and intersegmental force transmission in pathologic states.

Studies on contact biomechanics using in vitro methods have produced highly variable results and have become increasingly difficult to conduct due to ethical concerns and cost constraints. Consequently, in recent years, in vitro testing has gradually been replaced by Finite Element Analysis (FEA), a numerical simulation technique that offers a more controlled and cost-effective alternative [8]. Li and Wang have developed finite element models of the lumbar spine segment L1–L2, but their models often lacked anatomical realism, particularly in terms of material property differentiation among various bone structures [9]. Zulkifli further attempted lumbar simulation but focused solely on L2 without integrating the adjacent L1 vertebra, limiting intersegmental interaction analysis [10]. These limitations show a lack of studies that employ realistic bone material properties under multiaxial loads and investigate stress behavior in L1–L2 comprehensively.

The L1–L2 segment was selected for this study based on the clinical observation that the region marks the transition between the thoracic kyphosis and lumbar lordosis, thereby serving as the initial site of curvature in the lumbar spine during flexion. Consequently, it is particularly susceptible to stress accumulation, especially during the early phases of flexion and axial movement. This increased mechanical demand makes the region vulnerable to fracture under complex loading conditions [11]. Therefore, this study aims to investigate stress distribution on the L1/L2 endplates under multiaxial loads using FEA. The direction and magnitude of von Mises stress under various loading conditions were also determined. Regions of stress concentration on the superior and inferior endplates that may serve as indicators for mechanical failure risk were then identified. The results are expected to serve as a biomechanical reference for future studies involving degenerative conditions or intervention simulations. The current study addresses current gaps by providing detailed, load-specific stress maps for a healthy L1–L2 segment using anatomically informed models and multiaxial conditions, thereby enhancing the accuracy and clinical relevance of spinal biomechanics.

2. Materials and Method

A model of the lumbar spine, specifically at the L1 to L2 segment, was constructed based on imaging data from a healthy 55-year-old male respondent (66 kg, 168 cm). Clinical evaluations and imaging confirmed the absence of abnormalities, allowing for the development of a normal and anatomically accurate FE model. The respondent was recruited through the Spine Surgery Department at Dr. Kariadi Hospital, Semarang, after providing written informed consent. Ethical approval for this study was granted by the Ethics Committee (Approval No. 108/EC/KEPK/fk-UNDIP/IV/2022), according to institutional and national study guidelines.

Following image acquisition, the 3-dimensional geometry of the L1–L2 vertebral segment was reconstructed using Mimics 21.0 (Materialise, Belgium), a medical image processing tool capable of segmenting anatomical structures from CT data with high precision. The processed geometry was exported in STL format and subsequently imported into ANSYS Workbench 2023 R2 for preprocessing and simulation. In addition, the meshing process applied tetrahedral elements with local refinement in areas of complex geometry or expected stress concentration, balancing model accuracy with computational efficiency.

Kang *et al.* [12] reported that material properties were assigned to each anatomical structure in the model based on biomechanical parameters. These properties were selected to replicate the actual mechanical response of spinal tissues under physiological conditions, thereby ensuring the reliability of the model in predicting stress distributions and deformation patterns.

Key spinal ligaments were included to further improve the biomechanical fidelity of the model. These comprised the anterior longitudinal ligament (ALL), posterior longitudinal ligament (PLL), interspinous ligament (ISL), supraspinous ligament (SSL), ligamentum flavum (LF), intertransverse ligament (ITL), and capsular ligament (CL). The mechanical properties of these ligamentous structures were obtained from experimental data reported by Zewen Shi *et al*. [13], ensuring that their nonlinear and tension-dominant characteristics were properly reflected in the simulation. A summary of all material properties used in the model was presented in **Table 1**, including Young's modulus and Poisson's ratio for each component.

Table 1. Material properties of spinal components used in the finite element model

Material	Young Modulus (MPa)	Poisson's ratio
Bone Structures		
Cortical Bone	1200	0.3
Cancellous Bone	150	0.3
Endplate	1000	0.3
Posterior Structure	3500	0.3
Intervertebral disc		
Annulus	4.2	0.45
Nucleus	1	0.49
Ligaments		
Intertransverse Ligament	10	0.3
Supraspinous Ligament	8	0.3
Anterior Longitudinal Ligament	17	0.3
Posterior Longitudinal Ligament	10	0.3
Ligamentum Flavum	10	0.3
Interspinous Ligament	8	0.3
Capsular Ligament	15	0.3

The final geometry of the model was shown in **Figure 1**, which depicted the reconstructed and meshed L1–L2 segment ready for simulation. After material properties were assigned, boundary and loading conditions were applied to represent realistic physiological scenarios. The inferior surface of L2 was fully constrained in all degrees of freedom to simulate stabilization by the lower lumbar vertebrae and pelvic structure. Meanwhile, a vertical compressive load of 500 N was applied to the superior surface of L1, representing the upper body weight transmitted through the spine during standing posture.

Multiaxial moments of 2.5 N·m, 5 N·m, 7.5 N·m, and 10 N·m were applied to the superior surface of the L1 vertebra to simulate dynamic physiological movements such as bending and twisting. These moment loads were applied incrementally to represent a broad spectrum of spinal motions, including flexion, extension, lateral bending, and axial rotation, which were commonly encountered during daily activities such as lifting, turning, or bending forward. The selection of moment magnitudes was according to values reported in previous experimental and computational studies that reflected physiological and submaximal load conditions. This loading protocol was designed to investigate the mechanical response of the lumbar spine segment under combined axial and rotational stresses, which were known to significantly influence internal stress distributions and could contribute to degenerative changes or injury in susceptible individuals. The simulation results focused on the distribution of von Mises stress, allowing the identification of regions subjected to high mechanical loads and potential structural vulnerability under complex loading conditions.

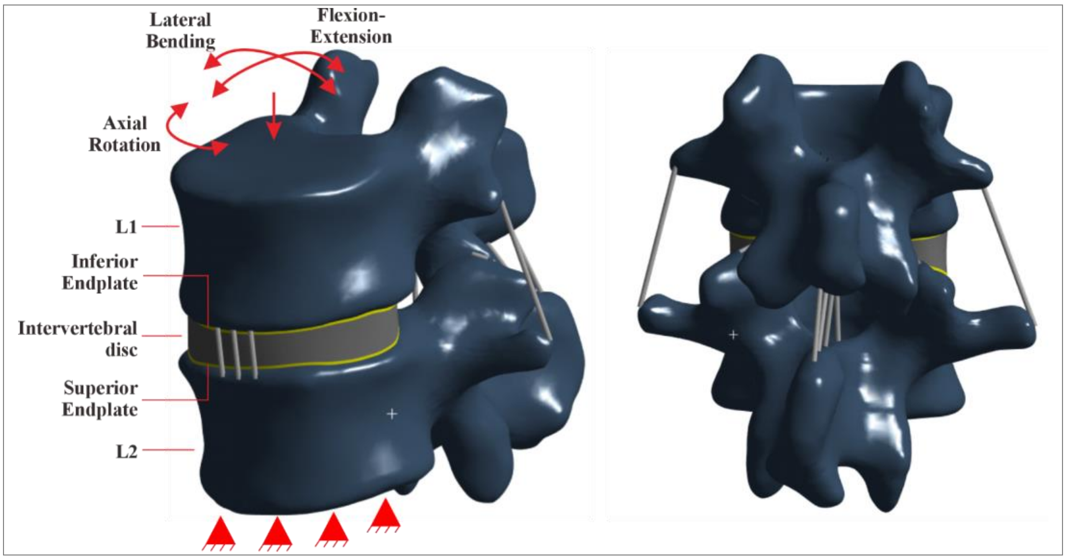

Figure 1. The reconstructed modeling of the L1–L2 lumbar vertebrae

3. Results and Discussion

3.1. Validation of FEM

To ensure the reliability of the developed FE model, validation was conducted by comparing the simulated displacement values with benchmark data from Li and Wang [9], under vertical loading conditions ranging from 500 N to 2500 N. The comparison focused on the L1 to L2 spinal segment, which was subjected to realistic multi-axial motions including flexion-extension, lateral bending, and axial rotation. These types of motion were commonly observed in daily activities such as bending down and twisting the torso to pick up an object from the side.

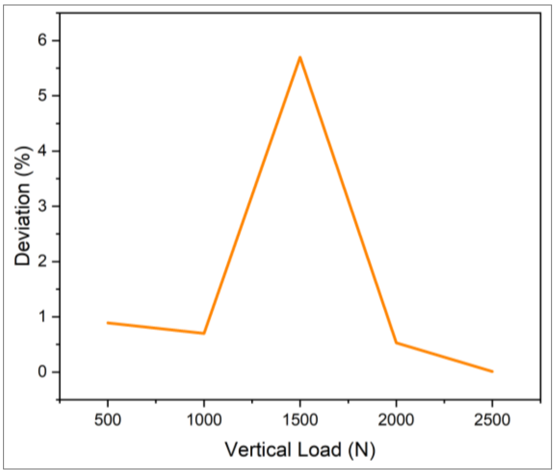

Figure 2. Percentage deviation between present study and Li & Wang [9]

As shown in **Figure 2**, the percentage deviation between this study and the reference data remained below 1 percent for most load conditions, indicating a strong agreement and validating the model's predictive capability. A slightly higher deviation of approximately 5.6 % was observed at 1500 N. This deviation could result from geometric sensitivity, mesh resolution, or simplifications in boundary conditions that were more influential at mid-range loading. Despite this, the overall trend of deviation was within acceptable limits for biomechanical simulations, supporting the credibility of the developed model.

Although the validation by Xu *et al*. [14] mainly focused on biomechanical parameters such as ROM, IDP, and FJF, their study considered simulation deviations up to 5 % as acceptable for mesh convergence. In some cases, even larger deviations were tolerated due to inherent variability in biological structures. Based on this precedent, the observed displacement deviation of 5.6 % at a single load point was considered acceptable and did not compromise the validity of the model. The validated displacement results confirmed that the FE model was capable of reproducing physiological motion behavior under vertical loading and could be used for further analysis under complex load conditions.

3.2. Endplate Stress of L1/L2 Segment

The lumbar spine, particularly the L1 to L2 segment, was subjected to complex multi-directional motions such as flexion-extension, lateral bending, and axial rotation daily. These movements were typically observed when an individual bent down and twisted the torso to retrieve an object from the side. To replicate these physiological loading conditions, a finite element simulation was performed using combined multiaxial loading that reflected typical human spinal movements. This approach aimed to evaluate the biomechanical response of the L1–L2 motion segment under realistic and functionally relevant loading scenarios.

The vertebral endplate played a significant role in transmitting loads and distributing stress across the intervertebral disc and vertebral body. In addition to its mechanical function, the endplate also contributed to nutrient transport and served as a protective structure for the disc [15]. Understanding its stress behavior under complex loads was therefore essential in evaluating spinal integrity.

Figure 3 illustrated the von Mises stress distribution patterns across the superior and inferior endplates of L1–L2 during combined motion. During extension and left axial rotation, von Mises stress appeared unevenly distributed, and peak stress zones shifted asymmetrically across the endplate surface. This finding indicated the inhomogeneous material properties of the endplate and the anatomical complexity of the vertebra, which resulted in nonlinear responses under combined loading. The inferior endplate, particularly its anterior region, experienced higher stress under these conditions, while the superior endplate showed broader stress dispersion toward the lateral regions.

When the extension moment increased, the von Mises stress on the endplate did not follow a proportional trend. Instead of increasing, the stress decreased, as shown in **Figure 4**. This observation suggested that the load was redistributed away from the disc and endplate toward more rigid spinal components such as cortical bone, and posterior ligaments [16], [17]. Such redistribution confirmed the spine's adaptive behavior, where various structural elements shared the mechanical load depending on the type and magnitude of movement.

This stress-shifting phenomenon supported the idea that the spine did not behave as a simple linear mechanical system. Rather, it served as an integrated and dynamic structure in which changes in 1 anatomical element influence the loading conditions experienced by others. As the extension moment increased, strain energy was redirected to stronger components such as cortical bone. Consequently, the endplate became less associated with load transmission. The analysis of lateral bending also revealed asymmetrical stress distribution. The superior endplate experienced

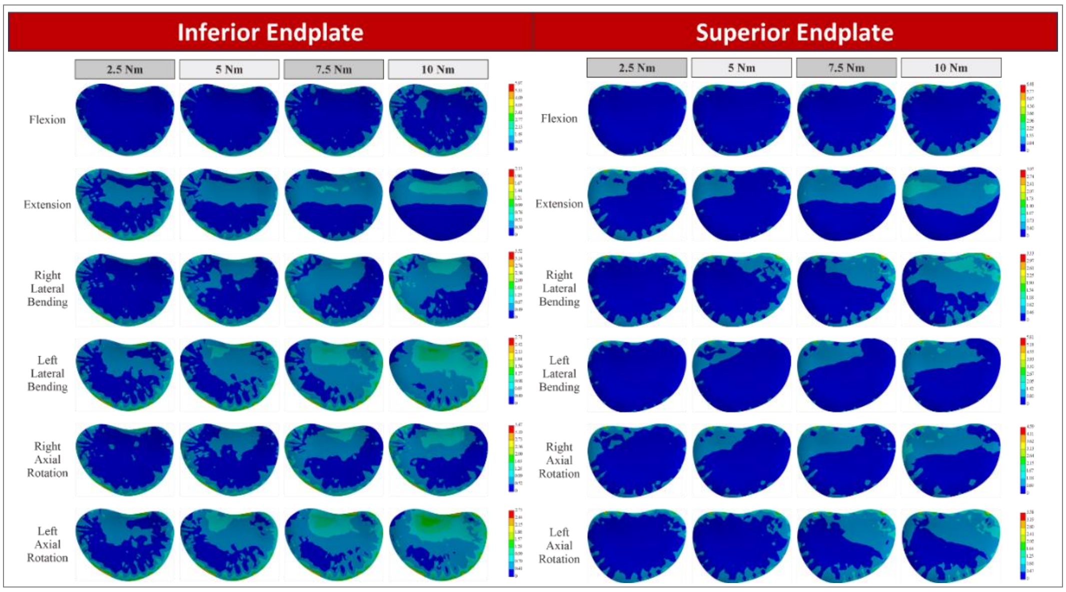

Figure 3. Von mises stress contours on superior and inferior endplates under multiaxial loading

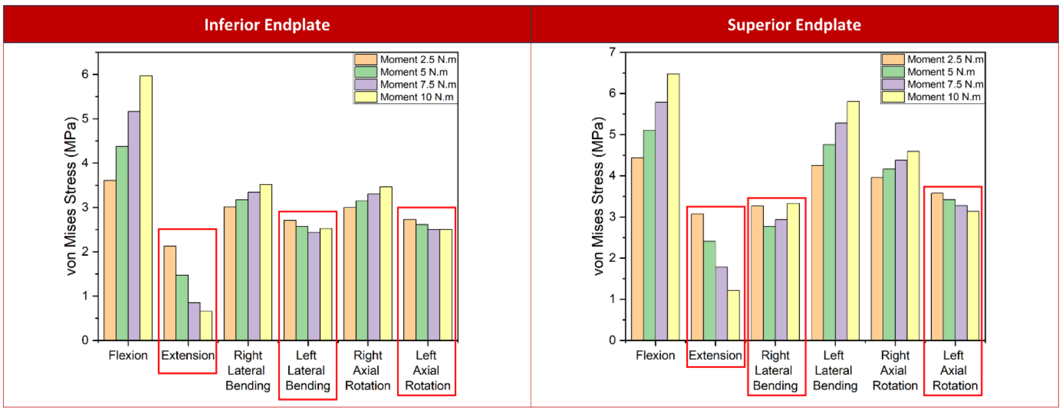

Figure 4. Data irregularities observed on the endplate

higher stress during left lateral bending, while the inferior endplate underwent higher stress during right lateral bending. This asymmetry likely resulted from natural anatomical differences such as cortical thickness, endplate geometry, and the orientation of trabecular bone between the left and right sides [18], [19]. The findings in this study were clinically important. During flexion and lateral bending in healthy individuals, the superior endplate consistently experienced higher von Mises stress compared to the inferior endplate. This condition suggested that the superior endplate could be more biomechanically vulnerable to pathological changes such as early-stage disc degeneration or compression fractures [20].

Simulation results provided further insight into stress behavior across spinal components under extension loading from 2.5 Nm to 10 Nm. The cortical bone of L1 showed a 93.97% increase in von Mises stress, rising from 13.957 MPa to 27.065 MPa, while L2 exhibited a 83.62% increase, from 28.642 MPa to 52.604 MPa. However, the superior endplate demonstrated a 60.54% decrease in stress, dropping from 3.0748 MPa to 1.2139 MPa, and the inferior endplate showed a 69.17% reduction, from 2.1323 MPa to 0.65713 MPa. Similarly, stress in the intervertebral disc components declined, the annulus fibrosus decreased by 67.60%, from 0.38106 MPa to 0.1235 MPa, and the nucleus pulposus by 70.02%, from 0.069891 MPa to 0.020956 MPa. These contrasting trends supported the hypothesis of load redistribution toward more rigid structures, particularly the cortical bone, during extension movement. These results emphasized the importance of incorporating stress distribution data into spinal implant design. Applying a stress-guided design approach reduced peak stress on vulnerable areas such as the superior endplate, especially during flexion and lateral bending. This design consideration was crucial to prevent microfractures or progressive damage, particularly in populations that were more susceptible to mechanical overload, such as elderly individuals or workers involved in heavy physical labor.

To reduce abnormal stress concentrations in daily activities, several preventive strategies were recommended. These included maintaining good posture while sitting or lifting, performing regular core-strengthening exercises to support spinal stability, and avoiding sudden or repetitive high-load movements. Nutritional interventions such as adequate calcium and vitamin D intake, along with regular bone density monitoring, were also essential for maintaining vertebral strength. For individuals with spinal degeneration or high biomechanical demands, assistive devices, such as passive exoskeletons could help distribute mechanical loads more evenly and reduce stress on the endplates [21].

In this study, numerical simulation data also supported this interpretation. The decrease in endplate stress despite increasing extension moment was consistent with the idea that load transfer transitioned to stronger structures such as cortical bone and facet joints [22], [23]. In addition, lateral bending exhibited a clear asymmetry. Higher stress was recorded on the superior endplate during left lateral bending and on the inferior endplate during right lateral bending. This behavior suggested that underlying differences in trabecular orientation or cortical thickness influence stress patterns, even when external loads were applied symmetrically.

Based on the findings derived from the simulation and data analysis, several limitations must be acknowledged, and directions for future studies were proposed to improve both academic and clinical relevance. This study was conducted using imaging data from a single respondent, which limited the generalizability of the findings. The anatomical characteristics and stress responses observed might not fully represent the diversity found in the broader population. Future studies must incorporate data from a larger and more varied sample to capture inter-individual differences in spinal geometry and biomechanical behavior.

The current model did not consider demographic and lifestyle factors such as age, gender, physical activity level, or occupational load. These variables played a significant role in influencing spinal mechanics and the development of degenerative conditions. Incorporating such parameters into future models could enhance their relevance to clinical applications and enable more personalized biomechanical assessments. Although this study revealed critical patterns of stress distribution relevant to spinal biomechanics, their direct application in implant design remained limited. Future work must explore stress-guided design approaches to develop spinal implants that promote physiological load sharing while maintaining structural stability. Such approaches could be particularly valuable for elderly patients or those with compromised bone quality, including individuals affected by osteoporosis or intervertebral disc degeneration.

4. Conclusion

In conclusion, simulation results indicated that vertebral endplates, particularly the superior endplate, played a significant role in load transmission and exhibited high-stress responses, especially during flexion and lateral bending. This led to their susceptibility to degeneration or fracture in this study. An increase in extension moment could reduce stress on the endplate, indicating a redistribution of load to stiffer structures such as cortical bone and posterior ligaments, emphasizing the adaptive and dynamic nature of the spinal system. These findings had important implications for the design of stress-distribution-based spinal implants to reduce the risk of microfractures, as well as supporting preventive strategies including core muscle strengthening, proper posture, and the use of assistive devices, such as passive exoskeletons to minimize abnormal loads on the endplate during daily activities.

Acknowledgements

The authors were grateful to all laboratory partners at the Undip Biomechanics Engineering and Research Centre (UBM-ERC) for their encouragement and valuable discussions regarding this study.

Authors' Declaration

Authors' contributions and responsibilities - The authors made substantial contributions to the conception and design of the study. The authors took responsibility for data analysis, interpretation, and discussion of results. The authors read and approved the final manuscript.

Funding – This work was granted by Diponegoro University in the scheme 609-122/UN7.D2/PP/VIII/2023 dan No. 609-122/UN7.D2/PP/VII/2024.

Availability of data and materials - All data is available from the authors.

Competing interests - The authors declare no competing interests.

Additional information – No additional information from the authors.

References

[1] M. I. Ammarullah *et al.*, "Tresca stress simulation of metal-on-metal total hip arthroplasty during normal walking activity," *Materials*, vol. 14, no. 24, p. 7554, 2021.

[2] M. I. Ammarullah *et al.*, "A review of enhanced total hip prosthesis design and material bearing combination to accommodate Muslim prayer (Salat) movements: Biomechanical, biotribological, and biological perspectives," *Tribology International*, vol. 205, no. January, p. 110518, 2025, doi: 10.1016/j.triboint.2025.110518.

[3] W. M. Park, K. Kim, and Y. H. Kim, "Effects of degenerated intervertebral discs on intersegmental rotations, intradiscal pressures, and facet joint forces of the whole lumbar spine," *Computers in Biology and Medicine*, vol. 43, no. 9, pp. 1234–1240, 2013, doi: 10.1016/j.compbiomed.2013.06.011.

[4] F. Galbusera and T. Bassani, "Lumbar spine biomechanics: A review of in vitro and computational studies," *Journal of Biomechanics*, vol. 94, pp. 73–83, 2019, doi: 10.1016/j.jbiomech.2019.07.004.

[5] Y. X. J. Wáng and others, "Osteoporotic vertebral endplate and cortex fractures: A pictorial review," *Journal of Orthopaedic Translation*, pp. 35–49, 2018, doi: 10.1016/j.jot.2018.08.004.

[6] R. Tsujimoto, H. Yamada, T. Nakazawa, T. Sugiura, and H. Ito, "Degenerative disc disease and osteophyte formation in lumbar spondylosis: A radiological and pathological correlation," *Spine Journal*, vol. 16, no. 5, pp. 679–687, 2016, doi: 10.1016/j.spinee.2016.01.012.

[7] I. Yamamoto, M. M. Panjabi, T. Crisco, and T. Oxland, "Three-dimensional movements of the whole lumbar spine and lumbosacral joint.," *Spine*, vol. 14, no. 11, pp. 1256–1260, Nov. 1989, doi: 10.1097/00007632-198911000-00020.

[8] R. Ismail *et al.*, "Design, fabrication, and performance testing of an energy storage and return (ESAR) foot prosthesis made of prepreg carbon composite," *Mechanical Engineering for*

Society and Industry, vol. 5, no. 1, pp. 20–32, Jan. 2025, doi: 10.31603/mesi.12652.

[9] H. Li and Z. Wang, "Intervertebral disc biomechanical analysis using the finite element modeling based on medical images," *Computerized medical imaging and graphics*, vol. 30, no. 6–7, pp. 363–370, 2006.

[10] A. Zulkifli, A. K. Ariffin, and M. M. Rahman, "Probabilistic finite element analysis of vertebrae of the lumbar spine under hyperextension loading," *International Journal of Automotive and Mechanical Engineering*, vol. 3, no. 1, pp. 256–264, 2011, doi: 10.15282/ijame.3.2011.3.0022.

[11] J. M. Daniels, C. Arguelles, C. Gleason, and W. H. Dixon, "Back Injuries," *Primary Care - Clinics in Office Practice*, vol. 47, no. 1, pp. 147–164, 2020, doi: 10.1016/j.pop.2019.10.008.

[12] S. Kang *et al.*, "Analysis of the physiological load on lumbar vertebrae in patients with osteoporosis: a finite-element study," *Scientific Reports*, vol. 12, no. 1, pp. 1–14, 2022, doi: 10.1038/s41598-022-15241-3.

[13] Z. Shi, J. Liu, X. Yu, L. Jiang, H. Wu, and Q. Pang, "The biomechanical effects of graded upper articular process arthroplasty on lumbar spine: A finite element study," *Journal of Orthopaedic Science*, vol. 25, no. 5, pp. 793–799, 2020, doi: 10.1016/j.jos.2019.10.012.

[14] M. Xu, J. Yang, I. H. Lieberman, and R. Haddas, "Lumbar spine finite element model for healthy subjects: development and validation," *Computer Methods in Biomechanics and Biomedical Engineering*, vol. 20, no. 1, pp. 1–15, 2017, doi: 10.1080/10255842.2016.1193596.

[15] K. B. Crump *et al.*, "Cartilaginous endplates: A comprehensive review on a neglected structure in intervertebral disc research," *JOR Spine*, vol. 6, no. 4, pp. 1–22, 2023, doi: 10.1002/jsp2.1294.

[16] M. Stańczak, M. Biały, and M. Hagner-Derengowska, "Ligament Cell Biology: Effect of Mechanical Loading," *Cellular physiology and biochemistry : international journal of experimental cellular physiology, biochemistry, and pharmacology*, vol. 59, no. 2, pp. 252–295, 2025, doi: 10.33594/000000773.

[17] Y. O. Özkılıç, "The capacities of thin plated stiffened T-stubs," *Journal of Constructional Steel Research*, vol. 186, 2021, doi: 10.1016/j.jcsr.2021.106912.

[18] J.-P. Roux *et al.*, "Contribution of trabecular and cortical components to biomechanical behavior of human vertebrae: An ex vivo study," *Journal of Bone and Mineral Research*, vol. 25, no. 2, pp. 356–361, 2010, doi: 10.1359/jbmr.090803.

[19] U. K. Ezemagu, F. Akpuaka, E. Iyidobi, and C. Anibeze, "Considering the surface area and sagittal angle in a pair of lumbosacral facets: Determining the structural relevance of asymmetric facets at the lumbosacral junction," *Journal of the Anatomical Society of India*, vol. 69, no. 4, pp. 237–242, 2020, doi: 10.4103/JASI.JASI_53_19.

[20] Y. Wang, H. Wang, F. Lv, X. Ma, X. Xia, and J. Jiang, "Asymmetry between the superior and inferior endplates is a risk factor for lumbar disc degeneration," *Journal of Orthopaedic Research*, vol. 36, no. 9, pp. 2469–2475, 2018, doi: 10.1002/jor.23906.

[21] V. Boddapati, F. Yuk, and S. Virk, "A Cadaveric Comparison of Discectomy Performance During Transforaminal Lumbar Interbody Fusion Approach Using an Endoscopic Technique Versus a Minimally Invasive Tubular Approach," *Spine*, vol. 50, no. 10, pp. 713–719, 2025, doi: 10.1097/BRS.0000000000005122.

[22] L. Zhang, H.-M. Li, R. Zhang, H. Zhang, and C.-L. Shen, "Biomechanical Changes of Adjacent and Fixed Segments Through Cortical Bone Trajectory Screw Fixation versus Traditional Trajectory Screw Fixation in the Lumbar Spine: A Finite Element Analysis," *World Neurosurgery*, vol. 151, pp. e447–e456, 2021, doi: 10.1016/j.wneu.2021.04.061.

[23] J. A. Guerrero-Vargas, P. Sanchez-Quinones, B. F. Pinzón, M. Vélez-Muriel, H. Madriñan-Navia, and L. Laverde-Frade, "The Role of Trabecular, Ligamentous-Intervertebral Disk and Facet Joints Systems: A Finite Element Analysis in the L4-S1 Vertebrae," *Global Spine Journal*, vol. 15, no. 2, pp. 1212–1228, 2025, doi: 10.1177/21925682241231525.